Hybrid silica-coated plasmonic-magnetic biomarkers

G.A. Sotiriou[*], A.M. Hirt[**], P-Y. Lozach[***], A. Teleki[*], F. Krumeich[*] and S.E. Pratsinis[*]

[*]Particle Technology Laboratory, sotiriou@ptl.mavt.ethz.ch
Institute of Process Engineering, Department of Mechanical and Process Engineering
[**]Institute of Geophysics, Department of Earth Sciences
[***]Institute for Biochemistry, Department of Biology
Swiss Federal Institute of Technology (ETH Zurich)
Sonneggstrasse 3, CH-9092, Zurich, Switzerland

ABSTRACT

Hybrid magnetic/plasmonic nanoparticles possess properties originating from each individual material. Such properties are beneficial for biological applications including bio-imaging, targeted drug delivery, *in vivo* diagnosis and therapy. Limitations regarding their stability and toxicity, however, challenge their safe use. Here, the one-step flame synthesis of composite SiO_2-coated Ag/Fe_2O_3 nanoparticles is demonstrated. The hermetic SiO_2 coating does not influence the morphology, the superparamagnetic properties of the iron oxide particles and the plasmonic optical properties of the silver particles. Therefore, the hybrid SiO_2-coated Ag/Fe_2O_3 nanoparticles exhibit desired properties for their employment in bio-applications.

Keywords: silver nanoparticles, iron oxide, silicon dioxide, bioimaging

1 INTRODUCTION

Plasmonic (Au or Ag) nanoparticles are superior markers for cell monitoring in bio-imaging, diagnosis [1] and therapy [2]. Such nanoparticles can be readily detected and traced by optical microscopy techniques such as dark-field illumination [3], two-photon fluorescence imaging [4], photon illumination confocal microscopy [5]. Alternatives to plasmonic nanoparticles for bio-imaging are the commonly used fluorescent organic dyes and semiconducting nanoparticles [6]. Fluorescent organic dyes, however, exhibit the so-called photobleaching and degrade during bio-imaging [7]. Semiconducting nanoparticles, on the other hand, exhibit optical blinking [8] while concerns arise for their toxicity as most contain cadmium or lead [6]. Even though plasmonic nanoparticles also induce toxicity [9], they are functionally advantageous over fluorescent organic dyes and semiconducting nanoparticles because they have superior photostability [10] and can be used also as photothermal therapeutic agents (e.g. tumor treatment) [5], offering an extra functionality in bio-applications.

When plasmonic nanoparticles are combined with another material, e.g. a magnetic component, multifunctional nanostructured materials are created [2], that can be detected and guided by multiple imaging and control techniques [11]. Magnetic resonance imaging (MRI) is an example of a traditional technique, with which small magnetic particles can be used as contrast agents [12] and for targeted drug delivery by directing them to organs, tissues or tumors using an external magnetic field or for magnetically-assisted cell sorting and separation [11]. Furthermore, a hermetic SiO_2 coating on the surface of such magnetic nanoparticles facilitates their surface bio-functionalization and prevents their magnetic particle-particle interaction and flocculation or agglomeration [13,14].

Composite plasmonic-magnetic nanostructures are typically made by multi-step wet methods. Usually, the magnetic particles are made first and act as a seeds for subsequent synthesis of plasmonic particles [2]. Depending on synthesis route, core/shell [15] or heterodimer [4] plasmonic-magnetic materials are formed. These "as-prepared" nanoparticles are often hydrophobic requiring a surface modification to suspend them in aqueous solutions [4]. Typically, the magnetic material is iron oxide (γ-Fe_2O_3 or Fe_3O_4) for its high spontaneous magnetization in a superparamagnetic state [11]. Imaging of live cells specifically bound to labeled composite Ag/Fe_3O_4 nanoparticles has been demonstrated [4], as they were magnetically manipulated by an external a magnetic field.

There are limitations, however, that hinder the use of such materials in bio-applications [16]. First and foremost, their toxicity needs to be addressed before they can be employed safely [16]. Even though Ag has the lowest optical plasmonic losses in the UV-visible spectrum [17], the more expensive Au nanoparticles are preferred for their lower cytotoxicity [9]. The release of toxic Ag^+ ions [18] when Ag nanoparticles are dispersed in aqueous solutions blocks their safe employment in bio-applications [19]. By coating Ag nanoparticles, however, with a nanothin, hermetic shell, this toxicity can be eliminated while their surface bio-functionalization can be enhanced by hindering also their flocculation [13] that poses another limitation in the use of plasmonic-magnetic nanomaterials [11,20] when dispersed in aqueous solutions. Overcoming these magnetic particle-particle interactions that result in their agglomeration or flocculation requires typically additional surface modification of these particles [2].

Here, one-step synthesis of hybrid, silica-coated, plasmonic-magnetic nanomaterials [21] is explored by scalable [22] flame aerosol technology. The morphology of these composite nanoparticles and the the plasmonic and magnetic properties of these hybrid nanoparticles are investigated.

2 EXPERIMENTAL

Silica-coated Ag/Fe_2O_3 particles were made in one-step with an enclosed flame aerosol reactor, described in detail elsewhere [13]. In brief, the composite core Ag/Fe_2O_3 nanoparticles were made by flame spray pyrolysis [23] of precursor solutions containing iron (III) acetylacetonate (Sigma Aldrich, purity ≥ 97%) and silver acetate (Sigma Aldrich, purity ≥ 99%) dissolved in 2-ethylhexanoic acid and acetonitrile (both Sigma Aldrich, purity ≥ 97%, volume ratio 1:1, stirring 100 °C for 30 minutes). The precursor solutions were fed at 5 mL/min to the FSP reactor and dispersed by 5 L/min O_2 forming a spray. The spray of the precursor solution (pressure drop 1.5 bar at the nozzle tip) was ignited by a ring-shaped, premixed methane/oxygen flame (1.5/3.2 L/min) and sheathed by 40 L/min O_2 (all gases Pan Gas, purity >99%). The Fe precursor concentration was kept constant at 0.5 M, while corresponding amounts of silver acetate were added to reach the nominal Ag wt%, which was defined as $x = m_{Ag}/(m_{Ag} + m_{Fe2O3})$, and called as Ag-content *x*. The freshly-formed composite Ag/Fe_2O_3 particles were coated in-flight by swirling injection of hexamethyldisiloxane (HMDSO, Sigma Aldrich, purity ≥99%) vapor along with 15 L/min nitrogen (PanGas, purity >99.9%) at room temperature through a metallic ring with 16 equidistant openings. The ring was placed on top of a 20 cm long quartz glass tube. The reactor was terminated by a 30 cm quartz glass tube. The HMDSO vapor was supplied by bubbling nitrogen through approximately 350 mL liquid HMDSO in a 500 mL glass flask. The SiO_2 amount was kept constant in the product particles and was calculated assuming saturated conditions [24] (bubbler temperature 10 °C and nitrogen flow rate 0.5 L/min) corresponding to 23 wt% for pure Fe_2O_3 core particles [14] (SiO_2 wt% = $m_{SiO2}/(m_{SiO2} + m_{Fe2O3})$). Silica-coated pure core Ag or Fe_2O_3 particles were made under identical conditions in the absence, however, of the corresponding precursor (Ag or Fe precursor).

High resolution transmission electron microscopy (HRTEM) was performed with a CM30ST microscope (FEI; LaB6 cathode, operated at 300 kV, point resolution ~2 Å) and scanning transmission electron microscopy (STEM) on a Tecnai F30 (FEI; field emission gun, operated at 300 kV). The electron beam could be set to selected areas to determine material composition by energy dispersive X-ray spectroscopy (EDXS; detector (EDAX) attached to the Tecnai F30 microscope). Product particles were dispersed in ethanol and deposited onto a perforated carbon foil supported on a copper grid. X-ray diffraction (*XRD*) patterns were obtained with a Bruker AXS D8 Advance spectrometer (Cu Kα, 40 kV, 40 mA). The crystallite size of silver and iron oxide was determined using the TOPAS 3 software and fitting only the main diffraction peaks. The optical properties of the composite particles were monitored with UV/vis spectroscopy (Cary Varian 500) of their aqueous suspensions. Magnetic measurements were made on a Princeton Measurements Corporation vibrating sample magnetometer (VSM), detailed elsewhere [25].

3 RESULTS AND DISCUSSION

3.1 Plasmonic-magnetic nanoparticles morphology

Figure 1a shows a high resolution TEM image of SiO_2-coated *10Ag/Fe$_2$O$_3$*. There is a single Ag nanoparticle (dark spot) attached onto Fe_2O_3 particles (gray). This indicates that Ag and Fe_2O_3 particles are closely attached to each other forming dumbbell- or Janus-like particles. There is an amorphous (light gray) SiO_2 shell or film encapsulating the core Ag/Fe_2O_3 particles of a couple of nm thickness [14]. EDX spectra measured over large areas of these samples reveal elemental compositions of Fe, Ag and Si that correspond to Fe_2O_3, Ag metal and SiO_2, respectively (Figure 1b). All STEM and TEM images indicate that there is no significant trace of individual or separate Ag or Fe_2O_3 particles, a pre-requisite for their bio-application. The average crystal size of the iron oxide nanoparticles was constant around 15 nm, while the silver varied from 10 to 25 nm for an increasing Ag-content.

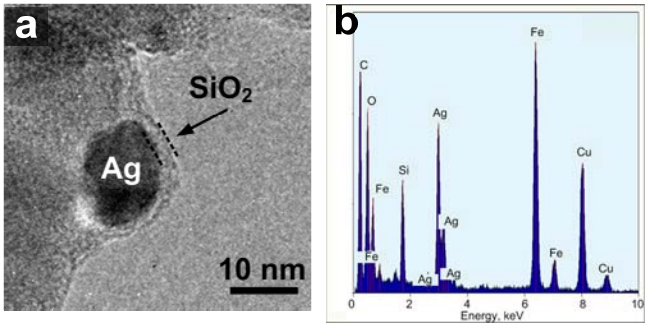

Figure 1. (a) TEM image of the SiO_2-coated *10Ag/Fe$_2$O$_3$* nanoparticles. (b) EDX analysis showing the elemental composition over a large area of the sample. Adopted from [21].

3.2 Plasmonic-Magnetic performance

Figure 2 shows the maximum magnetization of all hybrid plasmonic-magnetic particles (uncoated: triangles, SiO_2-coated: circles) normalized to their Fe_2O_3 mass at various Ag-contents *x* at room temperature. The magnetization stays almost constant for Ag-contents for Ag-contents 0-35 wt% while the SiO_2-coating does not influence their magnetic properties [14]. The highest magnetization (M_s = 39.4-46.1 emu/g) of the lower Ag-content particles (*x* = 6-35 wt%) is similar to pure Fe_2O_3

core (38.4 emu/g). These M_s values are lower than that of bulk γ-Fe_2O_3 (63.6 emu/g) [26], as smaller crystallites [14] are employed here that contain α-Fe_2O_3 (hematite) [26]. The slightly higher M_s for the low Ag-contents x = 6-35 wt% may be attributed to the slightly larger Fe_2O_3 crystal sizes in the presence of Ag as estimated from the XRD.

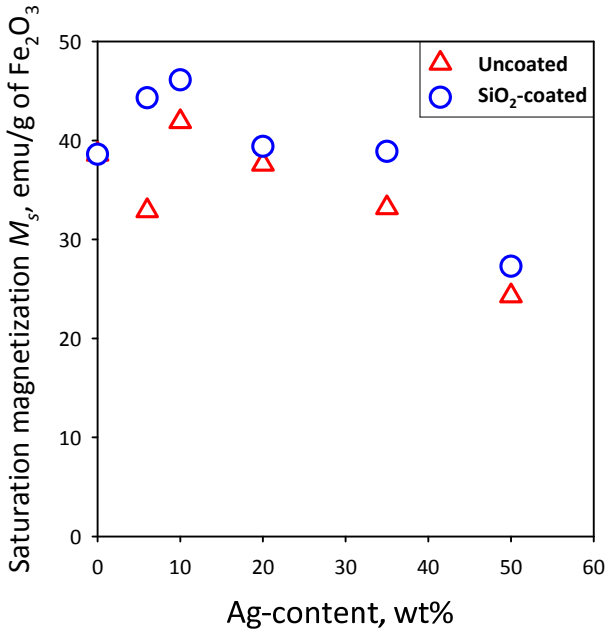

Figure 2. The sensor response Δλ as a function of time for the fully-coated (circles, diamonds) and partially-coated (squares, triangles) nanosilver. Adopted from [21].

Figure 3 shows the UV/vis absorbance of the uncoated hybrid particles here in aqueous suspensions. For the *10Ag/Fe_2O_3* the Ag-content is rather low and the Ag metal plasmon absorption band is not distinguishable. However, for an increasing Ag-content x > 10 wt% the plasmon band clearly emerges at ~400 nm and it is attributed to Ag metal [20]. This indicates that the optical properties of Ag nanoparticles are not influenced [27] by the presence of Fe_2O_3 nor SiO_2. Similar absorption spectra were obtained also for SiO_2-coated Ag/Fe_2O_3. Such particles could also be moved by a magnetic field. Therefore, these hybrid nanoparticles could be employed in bio-applications where both magnetic manipulation and optical monitoring are desired.

4 CONCLUSIONS

Hybrid, Janus- or dumbbell-like Ag/Fe_2O_3 nanoparticles are made and coated with a nanothin SiO_2 shell or film by one-step, scalable flame aerosol technology. These "as-prepared" nanoparticles were dispersible in water without any surface treatment. These particles exhibited near superparamagnetic behavior and their plasmon absorption band of Ag nanoparticles appeared clearly for an increasing Ag-content and size. This enables these nanoparticles to be employed in bioapplications where the optical properties of the plasmonic component as well as the magnetic properties of the iron oxide nanoparticles are desired, making them multifunctional probes.

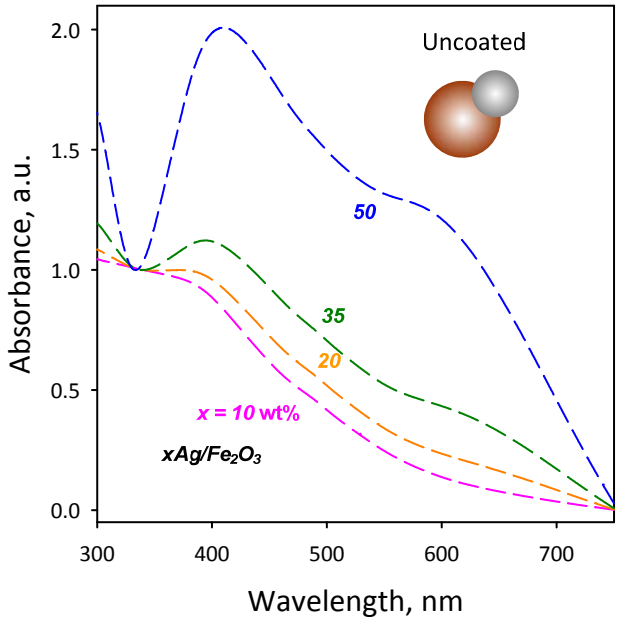

Figure 3. Optical absorption spectra of the uncoated Ag/Fe_2O_3 samples. The Ag plasmon band appears for an increasing Ag-content x, similarly to the SiO_2-coated Ag/Fe_2O_3 samples. Adopted from [21].

REFERENCES

[1] El-Sayed, I. H., Huang, X. H. & El-Sayed, M. A. Surface plasmon resonance scattering and absorption of anti-EGFR antibody conjugated gold nanoparticles in cancer diagnostics: Applications in oral cancer. *Nano Lett.* **5**, 829-834 (2005).

[2] Zeng, H. & Sun, S. H. Syntheses, properties and potential applications of multicomponent magnetic nanoparticles. *Adv. Funct. Mater.* **18**, 391-400 (2008).

[3] Aaron, J., Travis, K., Harrison, N. & Sokolov, K. Dynamic Imaging of Molecular Assemblies in Live Cells Based on Nanoparticle Plasmon Resonance Coupling. *Nano Lett.* **9**, 3612-3618 (2009).

[4] Jiang, J., Gu, H. W., Shao, H. L., Devlin, E., Papaefthymiou, G. C. & Ying, J. Y. Manipulation Bifunctional Fe_3O_4-Ag Heterodimer Nanoparticles for Two-Photon Fluorescence Imaging and Magnetic Manipulation. *Adv. Mater.* **20**, 4403-4407 (2008).

[5] Wang, C. G., Chen, J., Talavage, T. & Irudayaraj, J. Gold Nanorod/Fe_3O_4 Nanoparticle "Nano-Pearl-Necklaces" for Simultaneous Targeting, Dual-

Mode Imaging, and Photothermal Ablation of Cancer Cells. *Angew. Chem.-Int. Edit.* **48**, 2759-2763 (2009).

[6] Medintz, I. L., Uyeda, H. T., Goldman, E. R. & Mattoussi, H. Quantum dot bioconjugates for imaging, labelling and sensing. *Nature Mater.* **4**, 435-446 (2005).

[7] Das, G. K. & Tan, T. T. Y. Rare-earth-doped and codoped Y_2O_3 nanomaterials as potential bioimaging probes. *J. Phys. Chem. C* **112**, 11211-11217 (2008).

[8] Nirmal, M., Dabbousi, B. O., Bawendi, M. G., Macklin, J. J., Trautman, J. K., Harris, T. D. & Brus, L. E. Fluorescence intermittency in single cadmium selenide nanocrystals. *Nature* **383**, 802-804 (1996).

[9] Singh, S., D'Britto, V., Prabhune, A. A., Ramana, C. V., Dhawan, A. & Prasad, B. L. V. Cytotoxic and genotoxic assessment of glycolipid-reduced and -capped gold and silver nanoparticles. *New J. Chem.* **34**, 294-301 (2010).

[10] Lee, K. J., Nallathamby, P. D., Browning, L. M., Osgood, C. J. & Xu, X. H. N. In vivo imaging of transport and biocompatibility of single silver nanoparticles in early development of zebrafish embryos. *ACS Nano* **1**, 133-143 (2007).

[11] Lu, A. H., Salabas, E. L. & Schuth, F. Magnetic nanoparticles: Synthesis, protection, functionalization, and application. *Angew. Chem.-Int. Edit.* **46**, 1222-1244 (2007).

[12] Weissleder, R., Elizondo, G., Wittenberg, J., Rabito, C. A., Bengele, H. H. & Josephson, L. Ultrasmall superparamagnetic iron-oxide - Characterization of a new class of contrast agents for MR imaging. *Radiology* **175**, 489-493 (1990).

[13] Sotiriou, G. A., Sannomiya, T., Teleki, A., Krumeich, F., Vörös, J. & Pratsinis, S. E. Non-Toxic Dry-Coated Nanosilver for Plasmonic Biosensors. *Adv. Funct. Mater.* **20**, 4250-4257 (2010).

[14] Teleki, A., Suter, M., Kidambi, P. R., Ergeneman, O., Krumeich, F., Nelson, B. J. & Pratsinis, S. E. Hermetically coated superparamagnetic Fe_2O_3 particles with SiO_2 nanofilms. *Chem Mater.* **21**, 2094-2100 (2009).

[15] Lim, J., Eggeman, A., Lanni, F., Tilton, R. D. & Majetich, S. A. Synthesis and single-particle optical detection of low-polydispersity plasmonic-superparamagnetic nanoparticles. *Adv. Mater.* **20**, 1721-1726 (2008).

[16] Anker, J. N., Hall, W. P., Lyandres, O., Shah, N. C., Zhao, J. & Van Duyne, R. P. Biosensing with plasmonic nanosensors. *Nature Mater.* **7**, 442-453 (2008).

[17] Barnes, W. L., Dereux, A. & Ebbesen, T. W. Surface plasmon subwavelength optics. *Nature* **424**, 824-830 (2003).

[18] Navarro, E., Piccapietra, F., Wagner, B., Marconi, F., Kaegi, R., Odzak, N., Sigg, L. & Behra, R. Toxicity of silver nanoparticles to Chlamydomonas reinhardtii. *Environ. Sci. Technol.* **42**, 8959-8964 (2008).

[19] Schrand, A. M., Braydich-Stolle, L. K., Schlager, J. J., Dai, L. M. & Hussain, S. M. Can silver nanoparticles be useful as potential biological labels? *Nanotechnology* **19**, 235104-235117 (2008).

[20] Willets, K. A. & Van Duyne, R. P. Localized surface plasmon resonance spectroscopy and sensing. *Annu. Rev. Phys. Chem.* **58**, 267-297 (2007).

[21] Sotiriou, G. A., Hirt, A. M., Lozach, P. Y., Teleki, A., Krumeich, F. & Pratsinis, S. E. Hybrid, Silica-Coated, Janus-like Plasmonic-Magnetic Nanoparticles. *Chem Mater.* **in press**, DOI: 10.1021/cm200399t (2011).

[22] Mueller, R., Madler, L. & Pratsinis, S. E. Nanoparticle synthesis at high production rates by flame spray pyrolysis. *Chem. Eng. Sci.* **58**, 1969-1976 (2003).

[23] Madler, L., Stark, W. J. & Pratsinis, S. E. Simultaneous deposition of Au nanoparticles during flame synthesis of TiO_2 and SiO_2. *J. Mater. Res.* **18**, 115-120 (2003).

[24] Teleki, A., Heine, M. C., Krumeich, F., Akhtar, M. K. & Pratsinis, S. E. In situ coating of flame-made TiO_2 particles with nanothin SiO_2 films. *Langmuir* **24**, 12553-12558 (2008).

[25] Brem, F., Tiefenauer, L., Fink, A., Dobson, J. & Hirt, A. M. A mixture of ferritin and magnetite nanoparticles mimics the magnetic properties of human brain tissue. *Phys. Rev. B* **73**, 224427(224421-224426) (2006).

[26] Peters, C. & Dekkers, M. J. Selected room temperature magnetic parameters as a function of mineralogy, concentration and grain size. *Phys. Chem. Earth* **28**, 659-667 (2003).

[27] Gole, A., Agarwal, N., Nagaria, P., Wyatt, M. D. & Murphy, C. J. One-pot synthesis of silica-coated magnetic plasmonic tracer nanoparticles. *Chem. Comm.*, 6140-6142 (2008).